Progress In Electromagnetics Research M, Vol. 77, 115–123, 2019

Research on a Water-Immersed Wide Band Horn Antenna with Water-Filled Coaxial Impedance Matching Structure

Yang Yang[1], Lianghao Guo[1], Qing Zhou[1], Zhe Wu[1], Haibo Jiang[2], Zhongtuo Wang[1], Wenfei Bo[1], Jingchao Tang[1], Jialu Ma[1], Zhanliang Wang[1], Baoqing Zeng[1], and Yubin Gong[1, *]

Abstract—In order to improve the resolution of microwave biomedical imaging, a new method has been proposed in this paper, using a water-immersed wide band horn antenna at S-band. Considering the microwave penetration depth and the reflection at the interface between tissues and environment in deionized water, 2.45 GHz is selected as the central frequency of this antenna. Due to the high dielectric constant of water, the design of the impedance matching structure between the coaxial line and rectangular waveguide is most challenging. Therefore, the idea that using water as the medium of the coaxial impedance matching structure is proposed to deal with the problem of processing in our work. Simulated and experimental results show that this antenna has good impedance characteristics ($S_{11} < -10$ dB from 2.1 GHz to 3.8 GHz), good reasonable losses (5.1 dB total for two antennas and coaxial line at 3 GHz), and high maximum gain (8.52 dBi at 2.45 GHz).

1. INTRODUCTION

Microwave tomography is one of the new technologies which may have a potential use in biomedical imaging due to the ability to image the object possessing a complicated, nonlinear, high dielectric contrast inverse problem of diffraction tomography. Meanwhile, compared with the common imaging method, such as X-ray [1], nuclear magnetic resonance (NMR) [2], and ultrasonic imaging [3], microwave tomography (MWT) has the following advantages [4]. First, it is totally noninvasive as currently used tomographic systems. Second, the energy of "photons" in the microwave region is small enough to avoid ionization effects. Third, all tomographic systems for internal body imaging are based on the differentiation of tissue properties. So it has the ability to image bulk electrical properties as a feature of tissue that cannot be imaged by most other modalities. Finally, it can reconstruct frequency-dependent permittivity and conductivity profiles of living tissue quantitatively, without the use of contrast agents, as a way of identifying physiological conditions of those tissues.

However, what are some of the main problems hindering the applications of MWT imaging systems [5]? First, there is a contradiction between loss of incident electromagnetic wave signal and spatial resolution of the system. So microwave frequency [6] is usually selected between 1 and 4 GHz. Next, the incident signal will be greatly reflected at the interface between medium and tissues [7] leading to the signals inside the tissues too small. This problem can be well solved by encircling the tissues with the deionized water due to the suitable impedance matching between deionized water and tissues. Last, on the condition that the transmission loss and phase shift through a lossy dielectric are measured in a non-anechoic environment, the majority of the received signals by antennas may have not passed

Received 16 November 2018, Accepted 14 December 2018, Scheduled 2 January 2019
* Corresponding author: Yubin Gong (ybgong@uestc.edu.cn).
[1] National Key Lab on Vacuum Electronics, University of Electronic Science and Technology of China, Chengdu 610054, China.
[2] Chengdu Institute of Biology, Chinese Academy of Sciences, Chengdu 610041, China.

through the biological tissues due to multipath effect. Therefore, the biological tissues should be placed in an anechoic environment (such as water) to make high-quality measurements [8].

Above all, a water-immersed wide-band horn antenna with a water-filled coaxial impedance matching structure at S-band is proposed in this paper due to its appropriate size and frequency, the valid suppression of the reflection at the medium — target interface as well as higher resolution for biological imaging.

This paper is organized as follows. First, the attractive application prospects for nondestructive testing and evaluation of biological tissues using this antenna are discussed in the first part: Introduction. The structure of this water-immersed wide-band horn antenna is presented in the second part. Thirdly, S_{11}, S_{21}, 2-D and 3-D directivity pattern are calculated using the CST microwave studio [9]. The experimental results of S_{11}, S_{21}, 2-D directivity pattern at E-plane and H-plane are compared with that of simulation, which fits very well in the error range. Finally, some useful conclusions are given.

2. STRUCTURE OF THE ANTENNA

The geometry of the water-immersed wide-band horn antenna is presented in Fig. 1, and Table 1 gives the corresponding values of main parameters of this antenna. Here, the standard rectangular waveguide BJ220 with the length of 10.668 mm and width of 4.318 mm is selected. Since the working frequency range is from 17.6 GHz to 26.7 GHz in air, the corresponding frequency range is about 1.98 GHz to 3.02 GHz in water. The optimized height of the waveguide is about 5.2 mm.

Table 1. The corresponding values of the parameters of this antenna in Fig. 1.

Parameter	Value (mm)	Description
a_1	10.668	The length of the waveguide
a_2	20	The length of the aperture
b_1	4.318	The width of the waveguide
b_2	16	The width of the aperture
d_1	4	The width of the ridge
d_2	1	The rest width after chamfering at bottom of ridge
d_3	0.9	The distance between two ridges
d_4	3.118	The distance between two short ridge
l_1	2.759	The length of the first coaxial line of 8 Ω
l_2	3.46	The length of the second coaxial line of 8 Ω
l_3	18	The length of the coaxial line of 20 Ω
h_1	5.2	The height of the waveguide
h_2	16	The height of the flare
h_3	0.75	The height of the short ridge
h_4	3.2	The height of the feed

In virtue of the high dielectric constant of water whose average relative permittivity from 2 GHz to 4 GHz is about 77, its specific resistance value is about 43 Ω ($120\pi/\sqrt{77}$). It is hard to realize the matching transition from the coaxial line of 50 Ω to the water-immersed wide-band horn antenna directly. Therefore, the impedance matching between the coaxial line and rectangular waveguide will be most challenging in the design of this antenna.

As well known, the larger the size of the waveguide is, the larger impedance it has. Therefore, the impedance decreases gradually from the big mouth to the small mouth of the horn. Since the impedance of horn at the big mouth is about 43 Ω, the impedance at the small mouth will be too small to match with the coaxial line. It is necessary to design an impedance matching structure between the horn antenna and the coaxial line of 50 Ω, which is proposed and shown in Fig. 1(c). It can be seen that

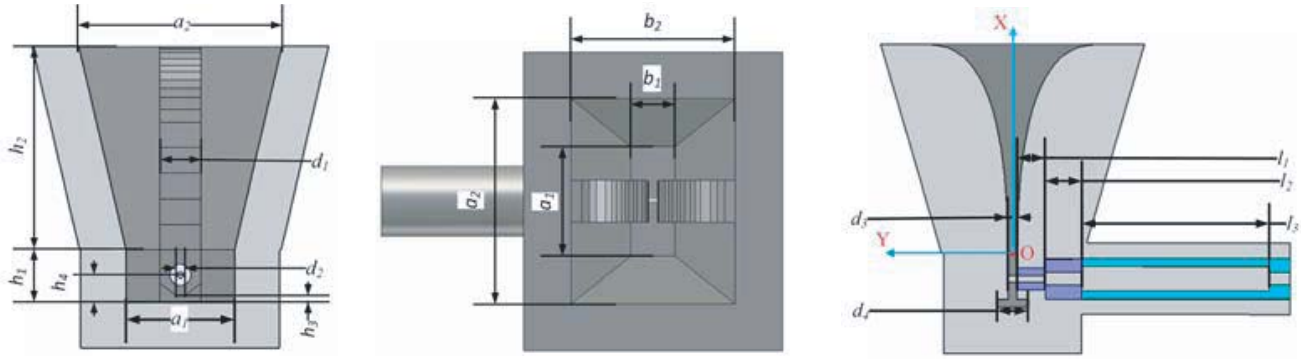

Figure 1. Geometry of the designed wide band horn antenna, (a) front view profile, (b) top view profile and (c) side view profile.

the coaxial line with the height of 3.2 mm can be divided into four sections, and the same impedance of the first two sections is 8 Ω with different lengths respectively 2.759 mm and 3.46 mm. In addition, the third section has the impedance of 20 Ω with a length of 18 mm while the fourth section is just the coaxial structure with an impedance of 50 Ω to match the universal long cable.

Based on the simplicity and operability of processing, the selection of medium of the coaxial structure and the design of the inner and outer diameters of medium of the coaxial structure mainly influence the performance of this antenna. The antenna has a better performance on condition that the diameter of the probe is about 0.64 mm and that the impedance of the first section of the coaxial structure is about 8 Ω. It is impossible to process this coaxial structure using a conventional bar as its medium. On the above account, the idea that using water as the medium of the coaxial structure is proposed to deal with the problem of processing in our work. Since the relative permittivity of water at 2.45 GHz is about 78.4, the outer diameter of first section of the coaxial structure is about 2.1 mm. The medium of the third section is Teflon ($\varepsilon_r = 2.2$), and the thickness of Teflon should not be too thin to be processed, so the inner diameter of 2.38 mm and outer diameter of 3.9 mm are selected. The second section is just an excessive structure between the first and third sections with the inner diameter of 1.2 mm and outer diameter of 3.9 mm.

The conventional double ridges structure with width of 4 mm is utilized to improve the frequency range of this antenna, as shown in Figs. 1(a), (b) and (c). The solution of ridge curve is a key part of ridge horn design, and it is usually an exponential curve, as shown in Fig. 2. Its mathematical form can be given by Equation (1) [10]:

$$Y(X) = Ae^{kX} + C \bullet X \tag{1}$$

where X represents the length of the ridge, and Y is the height of the ridge while A, C and k are related constants of the ridge curve.

It can be seen from Fig. 2 that the origin corresponds to the centre point O at the top of the

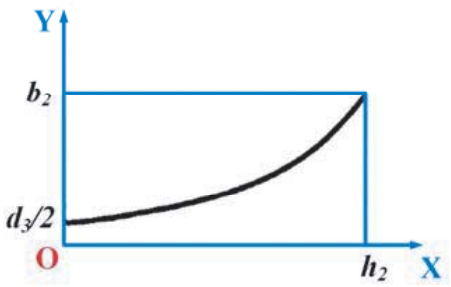

Figure 2. Diagram of the exponential ridge curve of this antenna.

waveguide in Fig. 1(c), which is marked in red. Based on the structure and corresponding parameters of this antenna in Fig. 1, the range of the values of X is from 0 to h_2, and the range of the values of Y is from $d_3/2$ to b_2.

The wave impedance at the exit of the horn antenna should be calculated strictly from the wave mode theory, but its calculation is very heavy [10, 11]. Therefore, a simplified design is necessary. The impedance at the exit of the horn antenna can be regarded as the wave impedance of water, and the water is equivalent to the terminal load of the horn antenna. The horn antenna itself can be considered as the impedance matching converter between the feed source and terminal load, and the double ridges play important roles for impedance matching. The impedance calculation of the double ridges in the rectangular waveguide can be found from [10, 11].

The impedances of this antenna at $X = 0$ and $X = h_3$ are respectively $8\,\Omega$ and $43\,\Omega$, and the impedance at $X = h_3/2$ can be approximately expressed as the average value of $8\,\Omega$ and $43\,\Omega$, which is just $25.5\,\Omega$. If substituting the above parameters into Equation (1), it is easy to get three simultaneous equations. Then, the values of A, k and C can be obtained. In addition, there are a short ridge at the

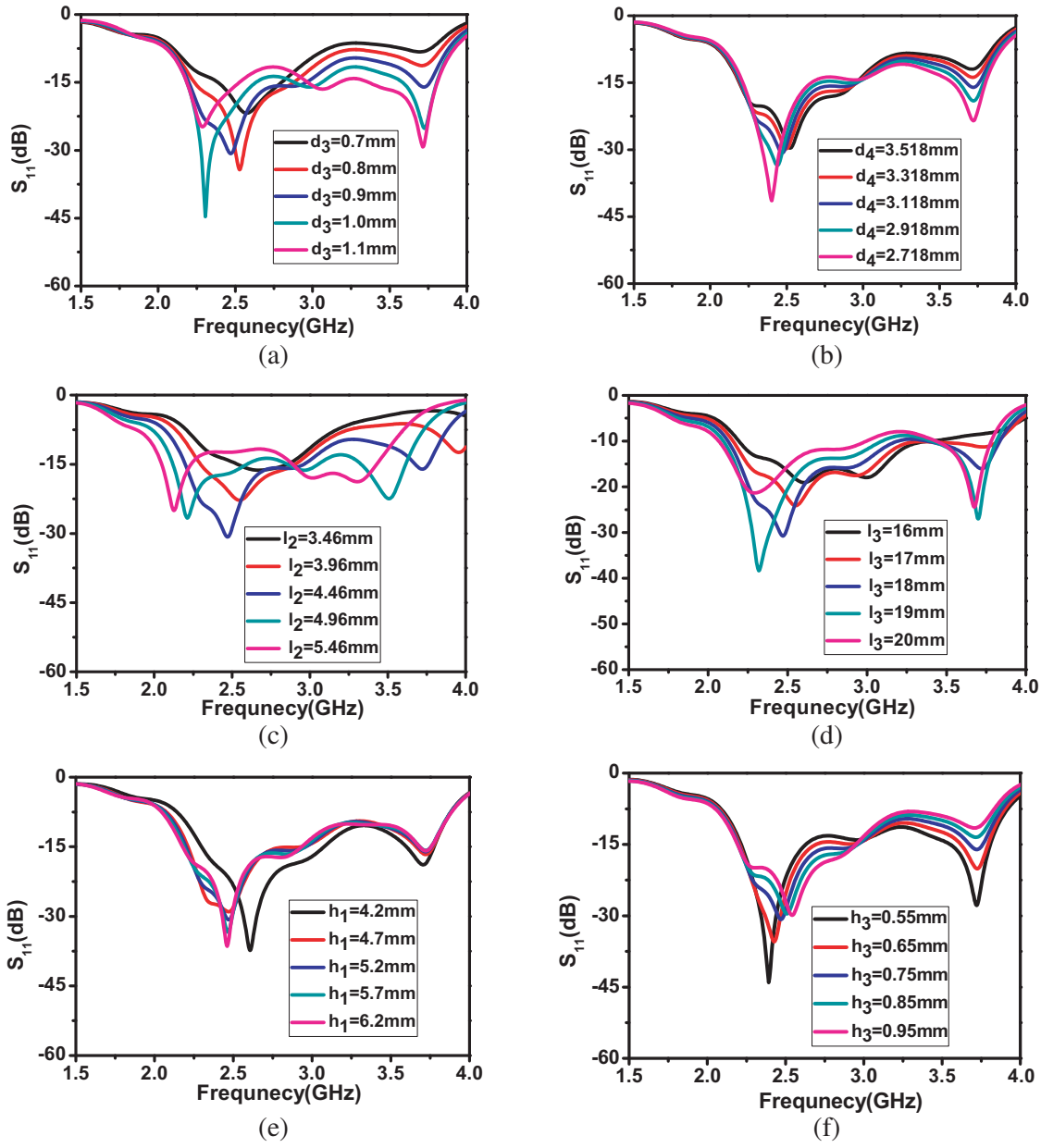

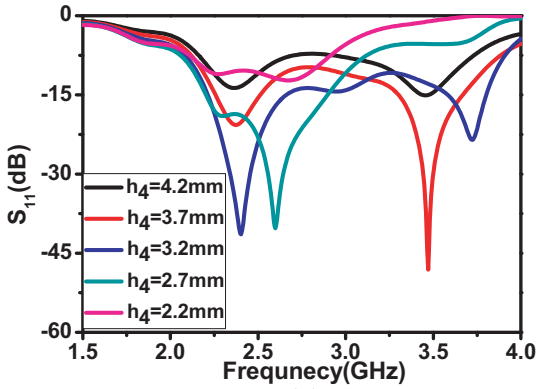

(g)

Figure 3. The influence on S_{11} of some important parameters (a) d_3, (b) d_4, (c) l_2, (d) l_3, (e) h_1, (f) h_3 and (g) h_4 respectively.

bottom of the waveguide and two chamfers at the bottom of the double ridges to realize good impedance matching and wide-band frequency range.

The performance of this antenna depends on lots of parameters, and the influences of some important parameters d_3, d_4, l_2, l_3, h_1, h_3 and h_4 on S_{11} are shown in Figs. 3(a), (b), (c), (d), (e), (f) and (g), respectively. It can be seen that the frequency increases as the d_3, l_2, l_3, h_4 and h_1 decrease while the frequency increases as the d_4 and h_3 increase. Based on the above situation, the values of these parameters in Table 1 are selected. Because the frequency changing with h_1 is not very obvious, and there is a very little difference among these simulation results, the middle value 5.2 mm of h_1 is a good choice. Of course, the value of h_1 from 4.7 mm to 6.2 mm can also be selected.

3. SIMULATION RESULTS AND EXPERIMENTAL RESULTS

This simulation is carried out by the CST microwave studio [9]. In the simulation model, as shown in Fig. 4, the operating frequency is from 1.5 GHz to 4 GHz. In order to calculate the microwave transmission loss in water, the surrounding medium of the structure during simulation is set as deionized

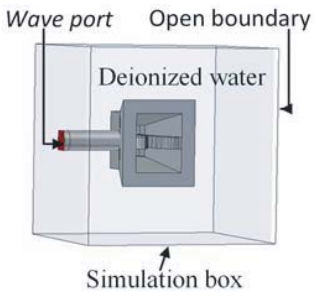

Figure 4. 3-D view of the simulation model and the installations of the medium, boundary and port.

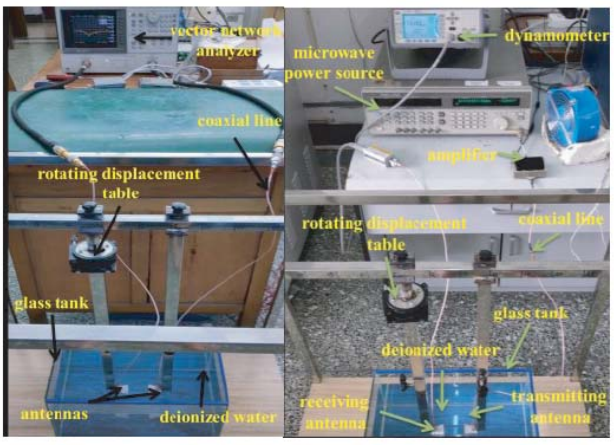

(a) (b)

Figure 5. The experimental configuration of (a) antenna transmission measurement and (b) antenna pattern measurement.

water, and all the components of this antenna are immersed in the deionized water. The coaxial line is perpendicular to the rectangular waveguide for generating the TE mode microwave signal, and the excitation signal is fed at the end of the coaxial line through a wave port. The open boundary is applied to the six surfaces of the box to make sure that the reflected wave totally vanishes.

To measure S_{11} of the single antenna and S_{21} between the two antennas, a set of swept transmission loss measurements were implemented [12]. As shown in Fig. 5(a), the tested antennas are placed at the center of the 40 cm × 24 cm × 35 cm glass tank (at the depth of 15 cm) filled fully with deionized water. Two designed antennas were fixed by two aluminum alloy supports, and there was an adjustable clamp at the end of the support to fix the antenna. Compared with the measurement in Fig. 5(a), the vector network analyzer is replaced by a group of measurement devices, which include a microwave power source, an amplifier of 20 dB, and an Agilent N1913A power meter shown in Fig. 5(b). The reasons are that water [5] is a very large lossy medium (382 dB/m at 3 GHz), and the energy of radiation signal received by another antenna will rapidly decrease as the angle increases. If the angle is large enough, the received signal will be too small to be extracted from the noise.

Figure 6 demonstrates the comparisons of S_{11} of the single antenna and S_{21} of two antennas with a distance of 5 mm and a distance of 50 mm submerged in deionized water between the experimental and simulation results. It can be seen that the experimental results S_{11} and S_{21} both agree with that of simulated results from 1.5 GHz to 4 GHz, and the $S_{11} < -10$ dB is from 2.1 GHz to 3.8 GHz, which shows a good performance of this wide-band horn antenna. However, there is a little difference between the center frequency of experiment and that of simulation. The reason is that the relative dielectric constant value of water in simulation from 2 GHz to 4 GHz may be different from the value of water used in experiment. The water in simulation is characterized by the first Debye mode [13–15], and the relative dielectric constant of water in simulation from 2 GHz to 4 GHz can be found in Fig. 6(c). Since

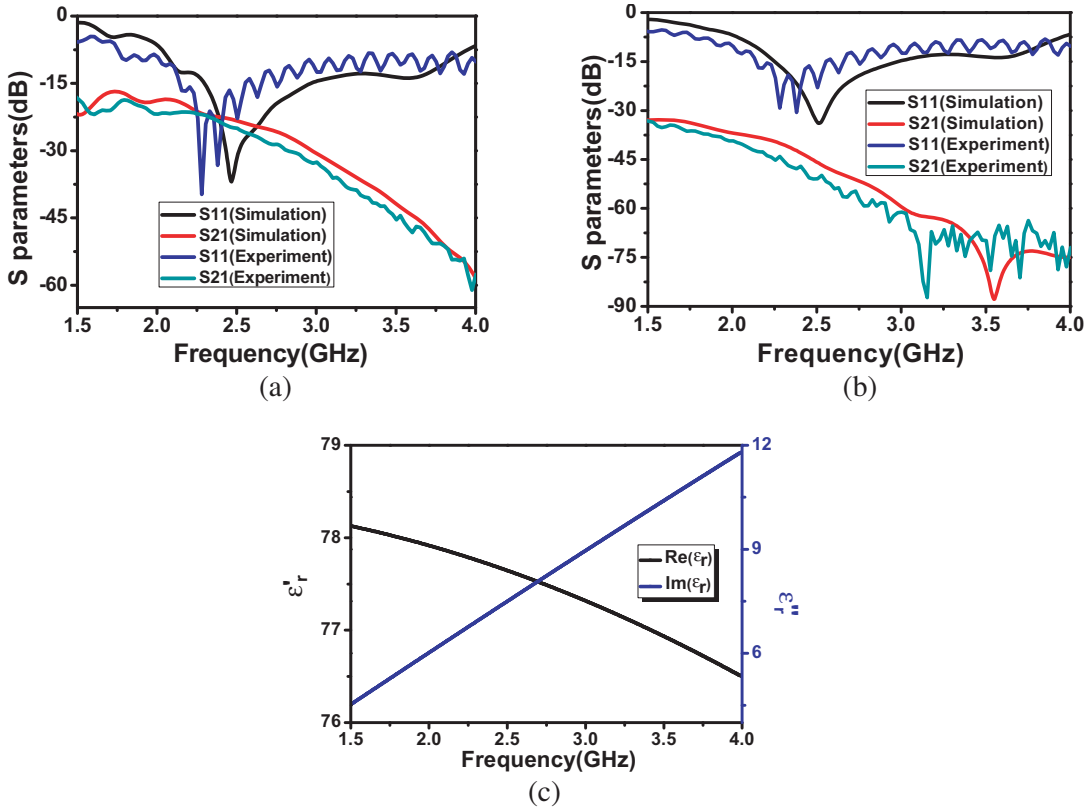

Figure 6. The simulated and experimental S_{11} of a single antenna, S_{21} of two antennas with a distance of (a) 5 mm, (b) 50 mm between them, (c) the relative dielectric constant of water from 1.5 GHz to 4 GHz using first Debye model.

polar liquid (like water) shows anomalous dispersion in radio frequency band, the refractive index and dielectric constant decrease as the frequency increases, which is called dielectric relaxation. According to above situation, Debye put forward the relaxation theory, which points out that the dipole orientation is hindered by intermolecular interaction and thermal motion under the action of external electric field. Therefore, the molecule of water can be regarded as a sphere in a continuous medium with macroscopic viscosity, which can be described by a viscous damping model (Debye mode). In addition, the relative dielectric constant of water in experiment is affected by the temperature and the conductive ion density in water. The real part of the relative dielectric constant of water varies with the temperature, which will result in the offset of center frequency. Meantime, the imaginary part of the relative dielectric constant of water will be bigger due to the bigger conductive ion density, which will lead to bigger transmission loss. The temperature and conductive ion density in experiment cannot be ensured absolutely same as that in simulation. It needs to be noticed that the little difference of center frequency (< 0.2 GHz) and transmission loss (< 8 dB) between experimental and simulated results is totally acceptable. From Fig. 6(a), S_{21} is about -32.57 dB at 3 GHz, subtracting the large loss (382 dB/m at 3 GHz) of water [5], which is about 27.4 dB (71.8 mm), the combined loss of two antennas and coaxial lines is just about 5.1 dB at 3 GHz. Meanwhile, the combined loss L can also be calculated by Equation (2):

$$L \approx (32.57 - 382 \times 0.0718)\,\text{dB} = 5.1\,\text{dB} \tag{2}$$

The 3-D directivity patterns at 2 GHz, 2.45 GHz and 3 GHz are presented in Figs. 7(a), (b) and (c), respectively. The box in the simulation of the far-field radiation is fully filled with pure water. Therefore, the simulation of the 3-D directivity pattern has not included the absorption loss in water. The maximum gains at 2 GHz, 2.45 GHz and 3 GHz are respectively 9.27 dBi, 8.52 dBi, and 10.3 dBi.

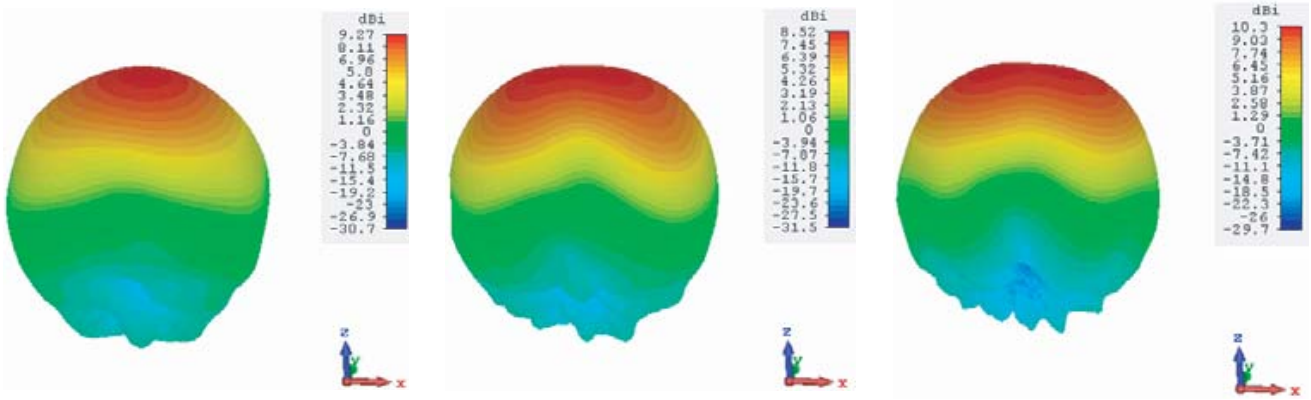

(a) (b) (c)

Figure 7. The simulated 3-D directivity pattern at (a) 2 GHz, (b) 2.45 GHz, (c) 3 GHz.

The simulated E-patterns and H-patterns at 2 GHz, 2.45 GHz and 3 GHz with the distance of 50 mm between two antennas are presented in Figs. 8(a) and (b), respectively, and the corresponding results of experiment are presented in Figs. 8(c) and (d). It can be seen that there is a big difference between the simulated results and experimental ones. The reason is that the simulation results have not included the absorption loss in water. The experimental 2-D radiation pattern in E-plate at 0 degree for 3 GHz is -39.019 dB, subtracting the 23 dB gain of amplifier, adding the 3.5 dB loss of the coaxial line, the 44.62 dB absorption loss in water (116.8 mm) [5] and the 33.07 dB transmission loss (50 mm) which is equal to $20\log(4\pi R/\lambda_g)$, then halving the calculated value, the experimental gain 10.641 dB of this antenna can be obtained. In addition, the gain G of one single antenna can be calculated by Equation (3):

$$G \approx (-39.019 - 23 + 3.5 + 20\log(4\pi \times 50/13.95) + 382 \times 0.1168)/2\,\text{dB} = 8.35\,\text{dB} \tag{3}$$

The value of the experimental gain agrees very well with that of simulation. In the same way, excluding the above interferential factors, the experimental results will be identical to simulated ones. Meanwhile, the experimental radiation gain decreases as the frequency increases, which just fits the variation tendency of the transmission lines in Figs. 6(a) and (b).

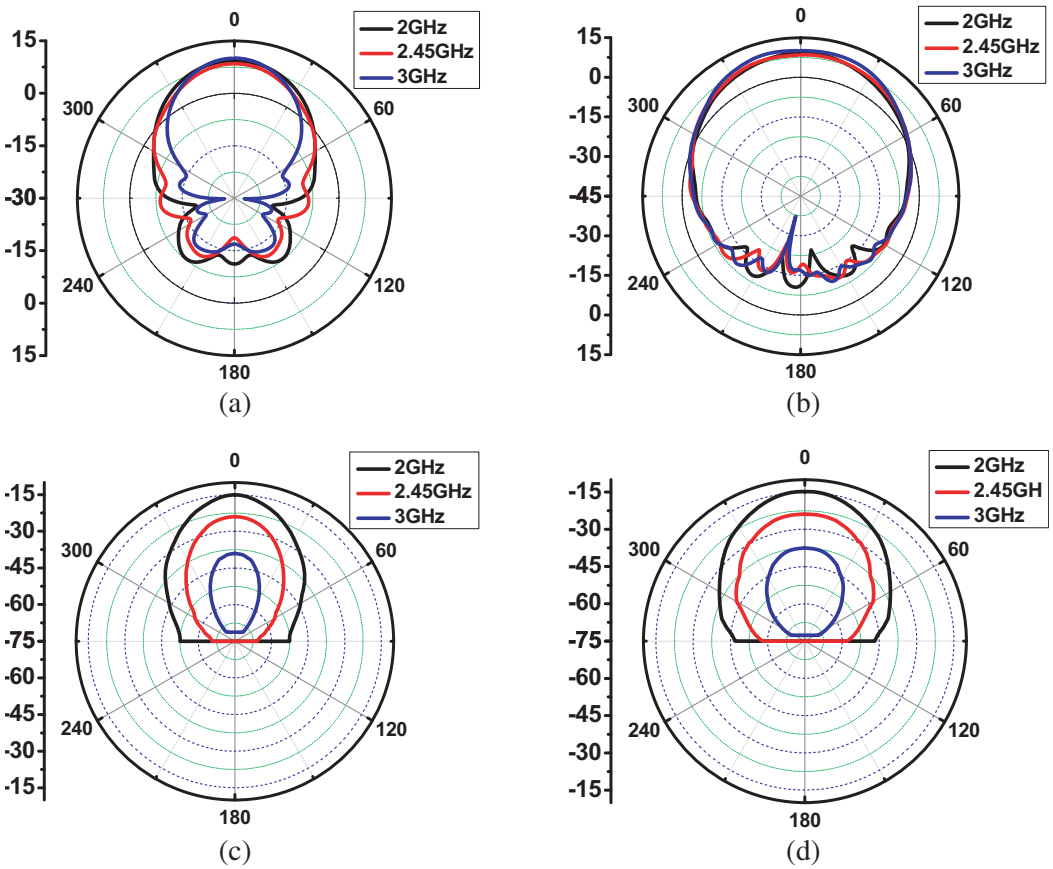

Figure 8. The simulated 2-D radiation pattern in (a) E-plate, (b) H-plate and the experimental 2-D radiation pattern in (c) E-plate, (d) H-plate at 2 GHz, 2.45 GHz and 3 GHz with the distance 50 mm between two antennas.

The simulated 3 dB angular widths in E-plate and H-plate are respectively 53.8 degree and 59.5 degree at 2 GHz, 47.9 degrees and 71.9 degrees at 2.45 GHz, 40.1 degrees and 72 degrees at 3 GHz, and the corresponding experimental 3 dB angular widths are respectively about 26 degrees and 37 degrees at 2 GHz, 29 degrees and 44 degrees at 2.45 GHz, 25 degrees and 38 degrees at 3 GHz. Although there is a difference between the simulated 3 dB angular width and that of experiment, their overall trends are generally the same. The reason for this difference may be that the loss of the microwave in water is different at different angles. The loss may increase as the angle increases due to longer transmission distance. In addition, there is a noise problem in weak signal detection, and the experimental results may include reflection of the glass and aluminum alloy at the larger angle. Based on the above reasons, the signal intensity detected by antenna may be smaller than that of truth at larger angle, resulting in a smaller 3 dB angular width in experiment.

4. CONCLUSION

In this paper, the experimental results show that it is practical to construct a horn antenna that operates at S-band while being completely submerged in water. Meanwhile, a water-filled coaxial impedance matching structure is proposed to make the antenna better match with the universal long cable of 50 Ω. This antenna has good impedance characteristics ($S_{11} < -10$ dB) from 2.1 GHz to 3.8 GHz, good reasonable losses (5.1 dB total for two antennas and coaxial line at 3 GHz), high gain far-field radiation, and large 3 dB angular width, which are all good enough to satisfy the requirements for biomedical imaging system.

ACKNOWLEDGMENT

This work was funded in part by the National Natural Science Foundation of China (Grant No. 61531010).

REFERENCES

1. Enander, B. and G. Larson, "Measurements of thermal electromagnetic radiation from the human body at microwave frequencies," TRITA-TET-7602, Division of Electromagnetic Theory, Tire Royal Institute of Technology, Stockholm, Sweden, Mar. 1976.
2. Gore, J. C. and Y. S. Kang, "Measurement of radiation dose distributions by nuclear magnetic resonance (NMR) imaging," *Physics in Medicine and Biology*, Vol. 29, No. 10, 1189, 1984.
3. Zhang, E., J. Laufer, and P. Beard, "Backward-mode multiwavelength photoacoustic scanner using a planar Fabry-Perot polymer film ultrasound sensor for high-resolution three-dimensional imaging of biological tissues," *Applied Optics*, Vol. 47, No. 4, 561–577, 2008.
4. Semenov, S. Y., R. H. Svenson, A. E. Boulyshev, et al., "Microwave tomography: Two-dimensional system for biological imaging," *IEEE Transactions on Biomedical Engineering*, Vol. 43, No. 9, 869–877, 1996.
5. Jacobi, J. H., L. E. Larsen, and C. T. Hast, "Water-immersed microwave antennas and their application to microwave interrogation of biological targets," *IEEE Trans. Microwave Theory Tech.*, Vol. 27, No. 1, 70–78, 1979.
6. Jofre, L., M. S. Hawley, A. Broquetas, et al., "Medical imaging with a microwave tomographic scanner," *IEEE Transactions on Biomedical Engineering*, Vol. 37, No. 3, 303–312, 1990.
7. Schwan, H. P., "Radiation biology, medical applications, andradiation hazards," *Microwave Power Engineering*, E. C. Okress (ed.), Vol. 2, 215–232, Academic, New York, 1968.
8. Yamaura, I., "Measurements of 1.8–2.7 GHz microwave attenuation in the human torso," *IEEE Trans. Microwave Theory Tech.*, Vol. 25, 707–710, Aug. 1977.
9. CST Studio Suite 2014, CST Computer Simulation Technology AG, Available at: www.cst.com.
10. Shao, Y. F., "A simplified design of wide band ridged horn antenna," *Modern Radar*, 2004 (in Chinese).
11. Chen, T. S., "Calculation of the parameters of ridge waveguides," *IRE Transactions on Microwave Theory & Techniques*, Vol. 5, No. 1, 12–17., 2003
12. Morabito, A. F., R. Palmeri, and T. Isernia, "A compressive-sensing-inspired procedure for array antenna diagnostics by a small number of phaseless measurements," *IEEE Transactions on Antennas and Propagation*, Vol. 64, No. 7, 3260–3265, 2016.
13. Meriakri, V. V. and E. E. Chigrai, "Determination of alcohol and sugar content in water solutions by means of microwave," *International Kharkov Symposium on Physics and Engineering of Microwaves, Millimeter, and Submillimeter Waves*, Vol. 2, 821–823, IEEE, 2004.
14. Liebe, H. J., G. A. Hufford, and T. Manabe, "A model for the complex permittivity of water at frequencies below 1 THz," *International Journal of Infrared & Millimeter Waves*, Vol. 12, No. 7, 659–675, 1991.
15. Peng, Y., "Numerical simulation of the dielectric properties of biological tissue in the terahertz band," Lanzhou Jiaotong University, 2015 (in Chinese).